

# Proxy-Based Sliding Mode Control: A Safer Extension of PID Position Control

Ryo Kikuuwe, *Member, IEEE*, Satoshi Yasukouchi, Hideo Fujimoto, and Motoji Yamamoto, *Member, IEEE*

**Abstract**—High-gain proportional–integral–derivative (PID) position control involves some risk of unsafe behaviors in cases of abnormal events, such as unexpected environment contacts and temporary power failures. This paper proposes a new position-control method that is as accurate as conventional PID control during normal operation, but is capable of slow, overdamped resuming motion without overshoots from large positional errors that result in actuator-force saturation. The proposed method, which we call proxy-based sliding mode control (PSMC), is an alternative approximation of a simplest type of sliding mode control (SMC), and also is an extension of the PID control. The validity of the proposed method is demonstrated through stability analysis and experimental results.

**Index Terms**—Position control, proportional–integral–derivative (PID) control, safety, saturation, sliding mode control (SMC).

## I. INTRODUCTION

THE DYNAMICS of robotic mechanisms are usually difficult to model due to the existence of many nonlinear factors, such as link inertia and joint frictions. To suppress the influence of such factors and disturbances, stiff position controllers are usually used as the lowest level controller. Low-level position controllers are necessary even for implicit force control [2] and admittance control [3]. The decentralized (independent joint) proportional–derivative (PD) and proportional–integral–derivative (PID) control schemes have been extensively used, especially for industrial robots, although there still remains theoretical challenge concerning the stability and the convergence property of the PID control [4]–[6].

One drawback of the stiff position control is that it can cause unsafe behavior when the desired position is far separated from the actual end-effector position. In such situations, the controller can produce excessively high speed to resume the desired position,

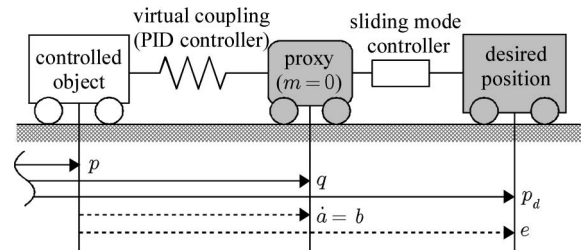


Fig. 1. Physical interpretation of PSMC.

tion, which usually results in overshoots and oscillations. Such unsafe situations occur in cases of unexpected environment contacts, temporal power failures to the actuators, discontinuous position commands from a higher level controller, etc. This kind of behavior is undesirable, especially with a robot that shares a common workspace with humans.

It is not a straightforward problem to eliminate such unsafe behaviors from a PID-controlled robot. Simple force limiters are not enough for this purpose because it does not explicitly guarantee slow, overdamped motion without overshoots. Another imaginable way is to use a very high velocity-feedback gain to produce a damped response. However, it will magnify the noise in the velocity measurements and will deteriorate the accuracy of position control during normal operation. Therefore, both accurate, responsive position control and slow, overdamped resuming motion cannot be achieved simultaneously by the conventional PID control.

This paper<sup>1</sup> proposes a *proxy-based sliding mode control* (PSMC) scheme that can produce slow, overdamped resuming motion after actuator-force saturation without sacrificing accurate, responsive tracking capability during normal operations. A physical interpretation of the scheme can be illustrated, as shown in Fig. 1. The actual controlled object is connected to a virtual object, which is referred to as a *proxy*, through a PID controller. The proxy is also connected to a sliding mode controller to track the given desired trajectory. The control algorithm of PSMC is the analytical solution for the differential algebraic constraints that result from this imaginary dynamical system. The algorithm can be viewed as an alternative approximation of conventional continuous-time sliding mode control (SMC), and also as an extension of PID control. The advantage of PSMC over the conventional PD and PID control is that the response to a large positional error, which results from actuator-force

Manuscript received April 5, 2009; revised September 29, 2009 and March 2, 2010; accepted May 17, 2010. Date of publication June 28, 2010; date of current version August 10, 2010. This paper was recommended for publication by Associate Editor A. Albu-Schäffer and Editor G. Oriolo upon evaluation of the reviewers' comments. This paper was presented in part at the 2006 IEEE International Conference on Robotics and Automation, Orlando, FL, May 15–19, 2006.

R. Kikuuwe and M. Yamamoto are with the Department of Mechanical Engineering, Kyushu University, Fukuoka 819-0395, Japan (e-mail: kikuuwe@ieee.org; yama@mech.kyushu-u.ac.jp).

S. Yasukouchi was with the Department of Intelligent Machinery and Systems, Kyushu University, Fukuoka 819-0395, Japan. He is now with the Yaskawa Electric Corporation, Kitakyushu 803-8530, Japan.

H. Fujimoto is with the Nagoya Institute of Technology, Nagoya 466-8555, Japan.

Color versions of one or more of the figures in this paper are available online at <http://ieeexplore.ieee.org>.

Digital Object Identifier 10.1109/TRO.2010.2051188

<sup>1</sup>This paper extends the authors' previous conference paper [1]. The authors have already published some papers [7]–[9] using the technique presented in this paper. This paper includes new concepts on continuous-time representations of the new controller, stability analysis, and new experimental results.

saturation, can be designed independently from the response to a small positional error that can be recovered without actuator-force saturation. In PSMC, the small-scale response can be set as fast as conventional PID or PD control, while the large-scale response can be set arbitrarily slow to ensure safety.

The rest of this paper is organized as follows. Section II prepares mathematical preliminaries, and Section III overviews the problem of conventional control laws, which also includes PD, PID, and SMC. The main contribution of this paper is presented in Section IV, in which the new control scheme is proposed. Section V describes stability analysis concerning the proposed control scheme applied to nonlinear robotic systems. Section VI presents experimental results. Section VII provides concluding remarks.

## II. MATHEMATICAL PRELIMINARIES

In the rest of this paper,  $\mathbb{R}$  denotes the set of all real numbers, and  $\mathbb{D}^n$  denotes the set of all  $n \times n$  diagonal matrices whose diagonal elements are all strictly positive. The symbol  $0$  denotes the zero vector or the zero matrix of appropriate dimensions. The symbol  $\|\cdot\|_p$  denotes the  $p$ -norm of the enclosed vector, while  $\|\cdot\|$  denotes the vector two-norm or the corresponding induced-matrix norm. The  $i$ th element of a vector  $z$  is denoted by  $z_i$ . The  $i$ th diagonal element of a diagonal matrix  $Z$  is denoted by  $Z_i$ .

Section IV will use the functions  $\text{sgn} : \mathbb{R} \rightarrow \mathbb{R}$  (signum function) and  $\text{sat} : \mathbb{R} \rightarrow \mathbb{R}$  (unit saturation function), respectively, which are defined as follows:

$$\text{sgn}(z) \begin{cases} = z/|z|, & \text{if } z \neq 0 \\ \in [-1, 1], & \text{if } z = 0 \end{cases} \quad (1)$$

$$\text{sat}(z) \triangleq \frac{z}{\max(1, |z|)}. \quad (2)$$

The set-valued form (1) is sometimes used in the literature, e.g., [10] and [11]. Although  $\text{sgn}$  is not a single-valued function, the equation-like expression  $y = \text{sgn}(z)$  is interpreted to be equivalent to the following logical expression:

$$\left( y = \frac{z}{|z|} \wedge z \neq 0 \right) \vee (|y| \leq 1 \wedge z = 0). \quad (3)$$

The derivation in Section IV intensively uses the following analytical relation between  $\text{sgn}$  and  $\text{sat}$ :

$$y = \text{sgn}(z - y) \iff y = \text{sat}(z) \quad \forall y \in \mathbb{R} \quad \forall z \in \mathbb{R}. \quad (4)$$

The proof of the relation is as follows:

$$\begin{aligned} y &= \text{sgn}(z - y) \\ \iff & (y = 1 \wedge z - y > 0) \vee (y = -1 \wedge z - y < 0) \\ & \vee (y \in [-1, 1] \wedge z - y = 0) \\ \iff & (y = 1 \wedge z > 1) \vee (y = -1 \wedge z < -1) \\ & \vee (y = z \wedge z \in [-1, 1]) \\ \iff & y = \text{sat}(z). \end{aligned} \quad (5)$$

The relation (4) can be illustrated as a pair of two equivalent block diagrams, as shown in Fig. 2. It implies that if the discontinuous function  $\text{sgn}$  is enclosed within a closed loop with-

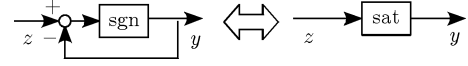


Fig. 2. Block-diagram representation of (4).

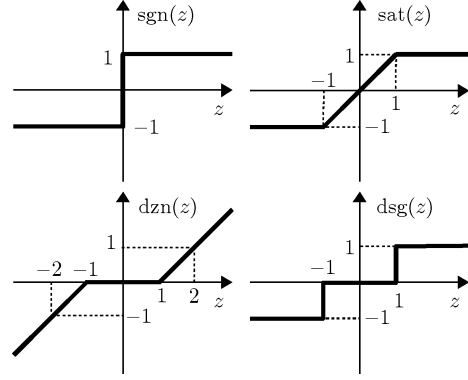


Fig. 3. Functions defined in Section II.

out latency, it can be removed with the use of the continuous function  $\text{sat}$ , which has no mathematical difficulty. As a direct consequence of (4), the following relations are convenient in the upcoming derivations:

$$y = Z \text{sgn}(Y(z - y)) \iff y = Z \text{sat}\left(\frac{z}{Z}\right) \quad (6)$$

$$\begin{aligned} y + Xw &= Y \text{sgn}(z - Zy) \\ \iff y &= -Xw + Y \text{sat}\left(\frac{(z/Z + Xw)}{Y}\right) \end{aligned} \quad (7)$$

where  $X, Y, Z > 0$ , and  $w, y, z \in \mathbb{R}$ . These relations hold true because of  $\text{sgn}(Zz) = \text{sgn}(z)$  for all  $Z > 0$  and  $z \in \mathbb{R}$ .

The analysis given in Section V will use the functions  $\text{dzn} : \mathbb{R} \rightarrow \mathbb{R}$  (dead-zone function) and  $\text{dsg} : \mathbb{R} \rightarrow \mathbb{R}$  (dead-banded signum function), respectively, which are defined as follows:

$$\text{dzn}(z) \triangleq z - \text{sat}(z) \quad (8)$$

$$\text{dsg}(z) \triangleq \begin{cases} z/|z|, & \text{if } |z| > 1 \\ 0, & \text{if } |z| \leq 1. \end{cases} \quad (9)$$

They satisfy  $d|\text{dzn}(z)|/dz = \text{dsg}(z)$ .

Fig. 3 illustrates the functions that are defined in this section. Besides, the element-wise vector versions of these functions are defined as follows:

$$\text{Sgn}(z) \triangleq [\text{sgn}(z_1) \quad \cdots \quad \text{sgn}(z_n)]^T \in \mathbb{R}^n$$

$$\text{Sat}(z) \triangleq [\text{sat}(z_1) \quad \cdots \quad \text{sat}(z_n)]^T \in \mathbb{R}^n$$

$$\text{Dzn}(z) \triangleq [\text{dzn}(z_1) \quad \cdots \quad \text{dzn}(z_n)]^T \in \mathbb{R}^n$$

$$\text{Dsg}(z) \triangleq [\text{dsg}(z_1) \quad \cdots \quad \text{dsg}(z_n)]^T \in \mathbb{R}^n$$

where  $z \in \mathbb{R}^n$ .

### III. CONVENTIONAL CONTROL LAWS

This paper considers  $n$ -degrees-of-freedom (DOF) rigid robot manipulators that can be described in the following form:

$$M(p)\ddot{p} + C(p, \dot{p})\dot{p} + D\dot{p} = f + h \quad (10)$$

where  $p \in \mathbb{R}^n$  denotes the vector of joint variables (angles for revolute joints and displacements for prismatic joints, respectively),  $f \in \mathbb{R}^n$  denotes the generalized force (torques for revolute joints and forces for prismatic joints) produced by the joint actuators,  $M(p) \in \mathbb{R}^{n \times n}$  denotes a symmetric positive-definite matrix that represents the inertia,  $C(p, \dot{p})\dot{p} \in \mathbb{R}^n$  denotes the centrifugal and Coriolis torques, and  $D \in \mathbb{D}^n$  denotes the coefficients of the viscous friction in the joints. The generalized force  $h \in \mathbb{R}^n$  denotes the sum of forces from all the external sources. It has been known that  $M(p)$  and  $C(p, \dot{p}) \in \mathbb{R}^{n \times n}$  are related by  $\dot{M}(p) = C(p, \dot{p}) + C(p, \dot{p})^T$  [12], [13]. The eigenvalues of  $M(p)$  are upper and lower bounded.

Most of the current industrial robots are actuated through high-ratio gear reducers to increase the available torque from actuators. The gear reducers also reduce the cross-coupling effects among the link inertias while preserving the effect of the rotor inertias. As a result, the contributions of the nondiagonal elements of  $M(p)$  and the vector  $C(p, \dot{p})\dot{p}$ , which are given in (10), become insignificant. Therefore, the dynamics of such a robotic system can be approximated by the following form:

$$M\ddot{p} + D\dot{p} = f + h \quad (11)$$

where  $p$  denotes the actuator angles,  $f$  denotes the torque produced by the actuators, and  $M \in \mathbb{D}^n$  is a constant diagonal positive-definite matrix. This means that the system is decomposed into  $n$  independent angle-control systems. The theoretical development in the paper will be mostly based on (11), although the analysis given in Section V will take into account the nonlinearity in (10).

#### A. Proportional–Derivative and Proportional–Integral–Derivative Control

For position control of robotic systems (10) or (11), PD control and PID control are the most popular methods because of their simplicity and robustness. As previously mentioned in Section I, they are not suited for the realization of both slow response against large positional error and accurate position control in normal operation. Low gains or low force limits are not suited for this purpose because they sacrifice accuracy and do not produce overdamped motion.

From a theoretical point of view, decentralized PD control with constant gains is proven to be useful for set-point control [14] of the system (10) with which global asymptotic stability is proven. The decentralized PD control is also useful for trajectory tracking, in which the desired position is not constant [15]–[17]. The addition of an integral term to a PD controller is a widely accepted way to eliminate steady-state offsets caused by gravity, Coulomb friction, and all other unmodelable forces. Stability of PID set-point control [6] and PID trajectory-tracking control [4], [5], [18], [19] has been shown under some inequality conditions, and the stability results are only local due to

the nonlinear term  $C(p, \dot{p})\dot{p}$ . Nevertheless, the influence of the nonlinear term is insignificant in geared robotic systems that can be approximated by (11). The effectiveness of PID control for the linear system (11) plus joint Coulomb friction has been theoretically supported, at least when there is no stiction (static friction being higher than kinetic friction) [20].

Many modifications have been proposed for PD and PID control schemes. Some of the saturated PID controllers are intended to guarantee global stability [12, Sec. 3.2] or semiglobal stability [21], [22]. Another class of modifications is for the prevention of abrupt behavior after discontinuous changes in the desired position command. Some researchers employ I-PD control [23], [24], in which the proportional and derivative feed-forward of the desired position command are removed. To ensure slow response, I-PD control sacrifices the responsiveness, which is necessary to maintain the tracking accuracy, even when the actuator forces are not saturated.

#### B. High-Gain Proportional–Derivative Control and Sliding Mode Control

It has been pointed out that a decentralized PD controller with very high gains decomposes the robotic system of the form (10) into two first-order subsystems: one being slow and the other being fast [25]. Specifically, let us consider the following control law:

$$f = K(p_d - p) + KH(\dot{p}_d - \dot{p}) \quad (12)$$

where  $p_d \in \mathbb{R}^n$  is the desired position vector, which is provided to the controller and  $K, H \in \mathbb{D}^n$ . As the proportional gains (the diagonal elements of  $K$ ) increase, the dynamics of the robot (10), under the control law (12), becomes more closely approximated by the following first-order dynamics:

$$p_d - p + H(\dot{p}_d - \dot{p}) = 0 \quad (13)$$

which can be obtained by substituting (10) by (12) and multiplying its both sides by  $K^{-1}$  (which is close to 0) from the left-hand side. Equation (13) represents the slow subsystem. The fast subsystem, on the other hand, acts to drive the state  $[p^T, \dot{p}^T]^T$  toward the manifold (13), as detailed in [25] in the light of singular perturbation analysis. This means that, even if the initial positional error  $(p_d - p)$  is large, (13) becomes satisfied after a short transient period, and after this, the system is governed by the dynamics (13), which exhibits overdamped convergence to the desired position  $p_d$  with the time constant  $H$ .

It has also been indicated that the high-gain feedback control has a close connection with SMC [25]–[27]. By considering limits on the magnitude of actuator forces and setting the proportional gains infinitely high, the control law (12) becomes equivalent to the following:

$$f = F \text{Sgn}(p_d - p + H(\dot{p}_d - \dot{p})) \quad (14)$$

where  $F \in \mathbb{D}^n$  is a diagonal matrix, whose diagonal elements are the magnitude limit of the  $i$ th actuator force, i.e.,  $|f_i| \leq F_i$ . This control law is a simple example of SMC that is presented in, e.g., [28, Sect. 6], although the controller in [28] includes

additional dynamics-compensating terms to ensure the global asymptotic stability. If  $F$  is set sufficiently high and if the nonlinear term in (10) is negligible, then the system state  $[p^T, \dot{p}^T]^T$  is attracted to the sliding manifold (13), as explained in [28]. After the manifold is reached, the system state develops according to the differential equation (13).

The aforementioned discussion implies that the high-gain PD control and the SMC are, in theory, capable of accurate tracking and slow overdamped response, which is the response characteristic aimed in this paper. It is, however, impossible to realize because the aforementioned theory depends on unrealistic assumptions of infinitely short sampling period, infinitely high gain, infinitely fast switching of the discontinuity in (14), and noiseless position and velocity measurements. Specifically, for the production of the aforementioned response characteristic, the proportional gains (the diagonal elements of  $K$ ) should be set as high as possible, and the time constants (those of  $H$ ) should be as large as, e.g., 0.1–1 s. Then, the derivative gain  $KH$  can become so high so as to magnify the noise in the velocity measurement. Although there are some filtering techniques to attenuate the discretization errors [29], there are inherent limits on the velocity feedback gain in practice. Moreover, high-gain velocity feedback will produce a slow response even to small positional errors, which deteriorate the tracking accuracy in normal operation.

The use of boundary layers around the discontinuity in the discontinuous function  $\text{Sgn}$ , given in (14), is a widely used remedy to attenuate chattering, which is a well-known drawback of the SMC. As discussed in [25], it makes the control law equivalent to the conventional PD controller with finite gains and force saturation.

Some researchers [30], [31] propose methods that combine PID control and SMC. In the Parra-Vega *et al.* [30] method, the integral of a discontinuous signum-type function of the positional error is used, and a reference position is exponentially moved toward the desired trajectory. In Lu's [31] method, the sliding manifold is also moved according to the integral of the positional error, but if the actuator force is saturated, it is exponentially moved without being influenced by the external forces. One shortcoming of such methods is that they do not consider the existence of unexpected external forces.

### C. Antiwindup and Reference Governor

One possible problem caused by the actuator-force saturation is the inconsistency between controller state variables and the controller output (i.e., the actuator forces). Such situations can result in unfavorable behaviors, which is referred to as “windup” problems, and techniques to prevent them are known as antiwindup techniques. There have been some frameworks of antiwindup techniques that can be applied to linear controllers [32]–[35]. In these frameworks, state variables in the controllers are modified so that they are kept consistent with the outputs, even when they are saturated. Another similar approach is reference governors [36], [37], with which the input to the controller is modified so that the system state and the controller output satisfy predetermined conditions.

There have been some antiwindup techniques specifically for PID controllers [38], [39]. These techniques are mainly for the reduction of the discrepancy between the saturated actuator force and the integrator in the PID controller. Such techniques do not provide direct solutions of the problem that is considered in this paper. This is because the undesirable behaviors of the PID-controlled robots, which are discussed in this paper, are not only attributed to the integrator windup; a robot can be unsafe even with PD control after a large positional error.

## IV. PROXY-BASED SLIDING MODE CONTROL

This section presents the new control algorithm that we named as PSMC. For simplicity, this section restricts itself to the 1-dimensional (1-D) case. The control algorithm is intended for the application as a joint-angle controller in decentralized position control, which are valid, at least, for robotic systems that are approximately linear and decoupled in the form of (11). The effect of nonlinearity, which appears in (10), will be analyzed in Section V.

This section starts with the derivation of the continuous-time representation of PSMC, which can be described by state and output equations. The continuous-time representation is useful for various analyses; however, it is not suitable for implementation. The actual control algorithm for implementation is derived on the basis of the backward (implicit) Euler discretization, which results in equations of different appearance.

As this section limits its scope to 1-D problems, all mathematical symbols in this section, such as  $f$  and  $K$ , are treated as scalars instead of vectors or matrices.

### A. Continuous-Time Proxy-Based Sliding Mode Control

The idea of PSMC can be understood with the use of the physical model illustrated in Fig. 1. In this model, the controlled object is connected to a virtual object (referred to as a *proxy*) through a virtual spring-like element (a *virtual coupling*) that performs a PID-type control action to maintain its length to be zero. The terms “proxy” and “virtual coupling” are borrowed from the area of haptic rendering [40]–[43]. The force exerted by the virtual coupling is sent to the actual actuator as a force command. The proxy accepts forces from the virtual coupling and from the another controller that performs a simple version of SMC to follow a desired position.

Let  $p \in \mathbb{R}$  and  $q \in \mathbb{R}$  denote the position of the controlled object and the proxy, respectively, and  $p_d \in \mathbb{R}$  denote a desired position for the controlled object. Then, the force  $f_{\text{PID}} \in \mathbb{R}$  produced by the PID-type virtual coupling can be written as follows:

$$f_{\text{PID}} = La + K\dot{a} + B\ddot{a} \quad (15)$$

where

$$a \triangleq \int (q - p) dt \quad (16)$$

and  $L$ ,  $K$ , and  $B$  are positive real numbers, which represent the integral, proportional, and derivative gains, respectively. These parameters should be appropriately chosen so that  $p$  is controlled

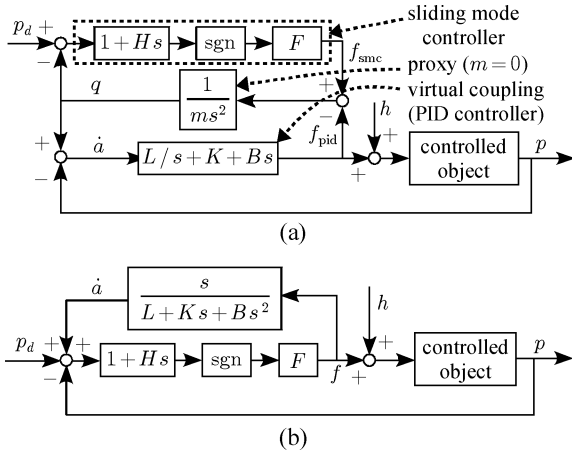


Fig. 4. Block diagrams of PSMC. Diagrams (a) and (b) are mutually equivalent.

to follow  $q$ . On the other hand, the force  $f_{\text{SMC}} \in \mathbb{R}$  from the controller on the other side is defined as follows:

$$f_{\text{SMC}} = F \text{sgn}(p_d - q + H(\dot{p}_d - \dot{q})) \quad (17)$$

where  $F > 0$ . The control law (17) is a simple SMC law, which appeared in (14) in Section III-B as an extreme case of PD control. Letting  $m$  be the proxy mass,  $m\ddot{q} = f_{\text{SMC}} - f_{\text{PID}}$  is satisfied. Fig. 4(a) shows the block diagram of the controller including  $m$ .

The proxy mass is set to be zero. Then,  $f = f_{\text{PID}} = f_{\text{SMC}}$  is satisfied, and (15) and (17) can be rewritten in the following form:

$$\sigma = p_d - p + H(\dot{p}_d - \dot{p}) \quad (18a)$$

$$0 = La + K\dot{a} + B\ddot{a} - F \text{sgn}(\sigma - \dot{a} - H\ddot{a}) \quad (18b)$$

$$f = La + K\dot{a} + B\ddot{a}. \quad (18c)$$

This is the continuous-time state-space representation of PSMC. Equation (18b) can be viewed as an implicit state equation concerning the state vector  $[a, \dot{a}]^T$ . Equation (18c) is the output equation that provides the actuator force  $f$ , which should be commanded to the actuator. It must be noted that Fig. 1 is not guaranteed to be a unique interpretation of (18).

Fig. 4(b) is a block-diagram representation of (18), although the causality between  $f$  and  $\ddot{a}$  is reversed in the expression. In Fig. 4, the  $\text{sgn}$  operator is enclosed within a closed loop in the controller. This can be rolled out as a  $\text{sat}$  function by using the rule of Fig. 2.

By the application of (7),  $\ddot{a}$  can be taken out of the discontinuous function  $\text{sgn}$ . Then, (18) can be rewritten as follows:

$$\sigma = p_d - p + H(\dot{p}_d - \dot{p}) \quad (19a)$$

$$\ddot{a} = -\frac{K\dot{a} + La}{B} + \frac{F}{B} \text{sat}\left(\frac{B}{F}\left(\frac{\sigma - \dot{a}}{H} + \frac{K\dot{a} + La}{B}\right)\right) \quad (19b)$$

$$f = F \text{sat}\left(\frac{B}{F}\left(\frac{\sigma - \dot{a}}{H} + \frac{K\dot{a} + La}{B}\right)\right). \quad (19c)$$

Note that (18) and (19) are algebraically equivalent. The equivalency implies that (18) is, in fact, a saturated controller, which does not include discontinuity and can have an explicit state equation. The discontinuous function in (18) does not produce discontinuity. This is the essential difference of PSMC (18), (19) from the sliding mode controller (14), which includes discontinuity that cannot be removed without approximation.

### B. Behavior of Proxy-Based Sliding Mode Control

An important feature of PSMC (18), or equivalently (19), is that it is an approximation of a sliding mode controller. By setting  $\hat{a} = Ka$  and  $\hat{L} = L/K$ , (18) can be rewritten as follows:

$$\sigma = p_d - p + H(\dot{p}_d - \dot{p}) \quad (20a)$$

$$0 = \hat{L}\hat{a} + \dot{\hat{a}} + \frac{B\ddot{\hat{a}}}{K} - F \text{sgn}\left(\sigma - \frac{\hat{a} + H\ddot{\hat{a}}}{K}\right) \quad (20b)$$

$$f = \hat{L}\hat{a} + \dot{\hat{a}} + \frac{B\ddot{\hat{a}}}{K} \quad (20c)$$

and by setting  $K \rightarrow \infty$ , (20) degenerates to

$$\sigma = p_d - p + H(\dot{p}_d - \dot{p}) \quad (21a)$$

$$\dot{\hat{a}} = -\hat{L}\hat{a} + F \text{sgn}(\sigma) \quad (21b)$$

$$f = F \text{sgn}(\sigma). \quad (21c)$$

Equation (21b) can be ignored because  $\hat{a}$  has no effect on the controller output  $f$ . Thus, as  $K \rightarrow \infty$ , the PSMC of (18) and (19) degenerates to (14), which is the simplest form of SMC, as discussed in Section III-B.

The controller (19) of PSMC can also be viewed as an extension of conventional control laws. By setting  $H = B/K$  and  $L = 0$ , (19) degenerates to

$$\sigma = p_d - p + H(\dot{p}_d - \dot{p}) \quad (22a)$$

$$\ddot{a} = -\frac{\dot{a}}{H} + \frac{F}{KH} \text{sat}\left(\frac{K\sigma}{F}\right) \quad (22b)$$

$$f = F \text{sat}\left(\frac{K\sigma}{F}\right), \quad (22c)$$

of which (22b) can be ignored because the state variable  $a$  has no effect on the controller output  $f$ . Thus, the controller (22) becomes equivalent to

$$f^* = K(p_d - p) + B(\dot{p}_d - \dot{p}) \quad (23a)$$

$$f = F \text{sat}\left(\frac{f^*}{F}\right) \quad (23b)$$

or equivalently

$$\sigma = p_d - p + H(\dot{p}_d - \dot{p}) \quad (24a)$$

$$f = \begin{cases} K\sigma, & \text{if } |\sigma| \leq F/K \\ F \text{sgn}(\sigma), & \text{if } |\sigma| > F/K. \end{cases} \quad (24b)$$

Equation (23) can be seen as the PD control with force saturation, while (24) can be seen as the SMC with a boundary layer [44], [45]. The equivalency of these two methods has been

pointed out in [46]. We can see that the PSMC of (18) and (19) is an extension of these conventional control schemes.

The behavior of a system under the PSMC of (18) and (19) can be understood by using  $q = p + \dot{a}$ , which can be interpreted as the proxy position that appears in Fig. 1. The position  $p$  of the controlled object always follows the proxy position  $q$  as the effect of the PID position controller (18c). When  $|f| < F$ , (18) implies  $0 = \sigma - \dot{a} - H\ddot{a}$  because, if not,  $|f| = F$  is necessary due to (18b) and (18c). By considering the definitions of  $\sigma$  and  $q$ , this is equivalent to

$$p_d - q + H(\dot{p}_d - \dot{q}) = 0, \quad (25)$$

which is the sliding surface incorporated in the sliding mode controller (17). From (25), if  $|f| < F$  is satisfied for all  $t \geq t_0$ ,

$$q = p_d + e^{-(t-t_0)/H} ((q - p_d)|_{t=t_0}) \quad (26)$$

is satisfied for all  $t \geq t_0$ . This means that, as long as  $|f| < F$ , the proxy position  $q$  exponentially approaches the desired position  $p_d$  with a time constant of  $H$ , without being influenced by any external disturbances. When  $|f| = F$ , on the other hand, the proxy is not on the sliding surface (25). This situation occurs, for example, when the robot yields to a large external force due to an actuator-force saturation.

Slow resuming motions from large positional errors are realized by setting  $H$  to be appropriately large. On the other hand, accurate trajectory tracking in normal operation is achieved by appropriate selection of the PID control gains  $K$ ,  $B$ , and  $L$ . In other words, an advantage of PSMC over conventional PID control is that the response against large positional errors and against small positional errors are independently designed. As PSMC is equivalent to PID control during  $|f| < F$ , the gain parameters  $K$ ,  $B$ , and  $L$  are tuned with the use of existing techniques, such as Ziegler–Nichols ultimate sensitivity method [47] and others [19]. The force limit  $F$  should be chosen by considering the tradeoff between the control performance (such as load-carrying capacity) and the safety. The time constant  $H$  can be chosen arbitrarily, and it only influences behaviors after saturation periods.

### C. Implementation: Discrete-Time Proxy-Based Sliding Mode Control

One important feature of the PSMC of (18) and (19) is that when  $|f| < F$ ,  $q = p + \dot{a}$  evolves according to (25), which is not influenced by physical disturbances that are propagated through  $p$ . For the implementation of PSMC to digital controllers, the state-space representation of (18) and (19) must be approximated by a discrete-time representation while strictly preserving this feature. The direct use of the explicit form (19) via a forward-Euler discretization is problematic because, in the forward-Euler implementation of (19b),  $\ddot{a}$  is computed according to  $\dot{a}$  of a timestep ago, and this results in (25) not strictly holding at each timestep.

One possible remedy is the use of backward (implicit) Euler discretization, with which (18) is rewritten as follows:

$$\sigma(k) = p_d(k) - p(k) + H \left( \frac{\nabla p_d(k)}{T} - \frac{\nabla p(k)}{T} \right) \quad (27a)$$

$$0 = La(k) + \frac{K\nabla a(k)}{T} + \frac{B\nabla^2 a(k)}{T^2} - F \operatorname{sgn} \left( \sigma(k) - \frac{\nabla a(k)}{T} - \frac{H\nabla^2 a(k)}{T^2} \right) \quad (27b)$$

$$f(k) = La(k) + \frac{K\nabla a(k)}{T} + \frac{B\nabla^2 a(k)}{T^2} \quad (27c)$$

where  $k$  is an integer that denotes a discrete-time index,  $T > 0$  is the time-step size, and  $\nabla$  denotes the backward-difference operator, which is defined as  $\nabla z(k) = z(k) - z(k-1)$ . It satisfies  $\nabla^2 z(k) = \nabla z(k) - \nabla z(k-1) = z(k) - 2z(k-1) + z(k-2)$ . Note that (27b) is an algebraic equation with respect to the unknown variable  $a(k)$ . To solve this, it is easier to replace the unknown  $a(k)$  by  $f(k)$  by using the following relation:

$$a(k) = \frac{(2B + KT)a(k-1) - Ba(k-2) + T^2 f(k)}{B + KT + LT^2}, \quad (28)$$

which is obtained from (27c). Then, (27b) can be rewritten as follows:

$$0 = f(k) - F \operatorname{sgn} \left( \frac{H + T}{B + KT + LT^2} (f^*(k) - f(k)) \right) \quad (29)$$

where

$$f^*(k) = \frac{B + KT + LT^2}{H + T} \sigma(k) + \frac{KH - B + LT(2H + T)}{(H + T)T} a(k-1) - \frac{KH - B + LTH}{(H + T)T} a(k-2). \quad (30)$$

Because of (6), (29) is equivalent to

$$f(k) = F \operatorname{sat} \left( \frac{f^*(k)}{F} \right). \quad (31)$$

Thus,  $f(k)$  is obtained as (31), and  $a(k)$  is subsequently obtained by using (28). In conclusion, the algebraic equations (27) can be solved with the use of the following computational procedure:

$$\sigma(k) = p_d(k) - p(k) + H \left( \frac{\nabla p_d(k)}{T} - \frac{\nabla p(k)}{T} \right) \quad (32a)$$

$$f^*(k) = \frac{B + KT + LT^2}{H + T} \sigma(k) + \frac{KH - B + LT(2H + T)}{(H + T)T} a(k-1) - \frac{KH - B + LTH}{(H + T)T} a(k-2) \quad (32b)$$

$$f(k) = F \operatorname{sat} \left( \frac{f^*(k)}{F} \right) \quad (32c)$$

$$a(k) = \frac{(2B + KT)a(k-1) - Ba(k-2) + T^2 f(k)}{B + KT + LT^2}. \quad (32d)$$

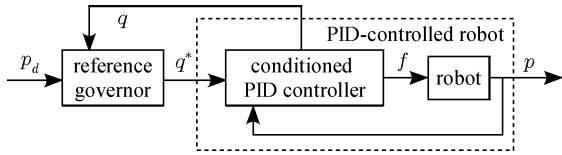


Fig. 5. Block diagram of (34). Another equivalent representation of PSMC.

This procedure is the discrete-time control law of PSMC, which can be directly implemented in digital, discrete-time controllers.

Setting  $L = 0$  with (32) results in a simpler procedure:

$$\sigma(k) = p_d(k) - p(k) + H \left( \frac{\nabla p_d(k)}{T} - \frac{\nabla p(k)}{T} \right) \quad (33a)$$

$$f^*(k) = \frac{B + KT}{H + T} \sigma(k) + \frac{KH - B}{H + T} b(k-1) \quad (33b)$$

$$f(k) = F_{\text{sat}} \left( \frac{f^*(k)}{F} \right) \quad (33c)$$

$$b(k) = \frac{Bb(k-1) + Tf(k)}{B + KT}. \quad (33d)$$

Here,  $b(k)$  corresponds to  $\nabla a(k)/T$ . The controller (33) can be viewed as the PD-version of PSMC. Although the controller (32) can be used even if  $L = 0$ , the controller (33) is preferred in this case to prevent numerical overflow in  $a(k)$ .

The discrete-time PSMC algorithm (32) can be viewed as a combination of a reference governor and a *conditioned* PID controller, which can be illustrated as Fig. 5. In fact, a tedious, but straightforward derivation shows that (32) is equivalent to the following algorithm:

$$q^*(k) = p_d(k) + \frac{H}{H + T} (q(k-1) - p_d(k-1)) \quad (34a)$$

$$a^*(k) = T(q^*(k) - p(k)) + a(k-1) \quad (34b)$$

$$f^*(k) = B \frac{a^*(k) - 2a(k-1) + a(k-2)}{T^2} + K \frac{a^*(k) - a(k-1)}{T} + La^*(k) \quad (34c)$$

$$f(k) = F_{\text{sat}} \left( \frac{f^*(k)}{F} \right) \quad (34d)$$

$$a(k) = \frac{(2B + KT)a(k-1) - Ba(k-2) + T^2 f(k)}{B + KT + LT^2} \quad (34e)$$

$$q(k) = p(k) + \frac{\nabla a(k)}{T}. \quad (34f)$$

Step (34a) can be viewed as a reference governor, which modifies the desired position  $p_d(k)$  to a new interim position  $q^*(k)$ . The position  $q^*(k)$  is achieved by the proxy if there is no force saturation. Steps (34b)–(34f) constitute the conditioned PID controller to track the desired position  $q^*(k)$  as long as the force  $f^*(k)$  does not exceed  $F$ . If it does exceed  $F$ , a modified proxy position  $q(k)$  is chosen by using (34e) and (34f) so that it produces the force of the marginal level  $F$  by satisfying the standard PID control law (27c) in a similar manner as the con-

ditioning techniques in [32] and [33]. The value  $q(k)$  is chosen equal to  $q^*(k)$  if  $|f^*(k)| \leq F$ . The new proxy position  $q(k)$  is sent to the reference governor (34a) in the next timestep.

By setting  $H = 0$ , the PSMC algorithm (32) becomes equivalent to the algorithm (34b)–(34f) with  $q^*(k)$  being replaced by  $p_d(k)$ . This means that, by setting  $H = 0$ , PSMC degenerates to a force-bounded PID controller with a particular kind of saturation behavior. If the initial positional error  $p_d - p$  is large, then the force  $f$  is kept saturated until  $p$  becomes close to  $p_d$ , while the internal variable  $a$  is kept consistent with  $f$ .

## V. ANALYSIS

This section provides a theoretical justification for the application of PSMC to independent joint-angle control of the robotic systems (10) and (11). As shown in Section IV, PSMC is an implicit combination of a PID controller and a sliding mode controller. This structure is motivated by the empirical fact that a well-tuned PID controller is effective for trajectory tracking. However, there is no standard ways to exhibit the theoretical validity of PID trajectory-tracking control. Thus, this section will introduce a conjecture that a well-tuned PID-controlled robot is strictly passive as long as the magnitude of the nonlinear term in (10) is low enough. Under this conjecture, it will be shown that the joint angles converge to the neighborhood of the desired values.

In this section, variables such as  $f$  and  $K$  can be vectors and matrices, as defined in Section III and as will be defined in this section.

### A. Dynamics of Robot and Controller

This section considers the robotic system (10) and its linear approximation (11). Let  $p_d \in \mathbb{R}^n$  be the vector of desired joint angles, and  $e \in \mathbb{R}^n$  be the joint-variable error vector that is defined as  $e \triangleq p_d - p$ . For the convenience of upcoming derivations, let us define the following vectors:

$$x \triangleq [e^T \quad x_e^T]^T \in \mathbb{R}^{4n} \quad (35)$$

$$x_e \triangleq [e^T \quad \dot{a}^T \quad a^T]^T \in \mathbb{R}^{3n}. \quad (36)$$

Let us assume that  $\|\ddot{p}_d\|$ ,  $\|\dot{p}_d\|$ , and  $\|h\|$  are upper bounded.

Substituting (10) by  $p = p_d - e$  yields the following:

$$M(p)\ddot{e} + (C(p, \dot{p}) + D)\dot{e} = -f + \phi \quad (37)$$

where

$$\phi \triangleq M(p)\ddot{p}_d + (C(p, \dot{p}) + D)\dot{p}_d - h \in \mathbb{R}^n, \quad (38)$$

which is the error-coordinate representation of the nonlinear robotic dynamics (10). Then,  $\|\phi\|$  satisfies

$$\|\phi\| < \alpha_0 + \gamma_v \|C(p, \dot{p})\| \quad (39)$$

where  $\alpha_0$  is a positive scalar, and  $\gamma_v$  is the upper bound of  $\|\dot{p}_d\|$ . For the linear approximation (11),  $\|\phi\|$  is bounded by  $\alpha_0$  because  $\|C(p, \dot{p})\| = 0$ .

The multidimensional version of PSMC (18) applied to each joint of the robot (37) can be described by the following

state-space representation:

$$s = e - \dot{a} + H(\dot{e} - \ddot{a}) \quad (40a)$$

$$0 = La + K\dot{a} + B\ddot{a} - F \text{Sgn}(s) \quad (40b)$$

$$f = La + K\dot{a} + B\ddot{a} \quad (40c)$$

where  $f, a, e \in \mathbb{R}^n$ , and  $K, B, L, F, H \in \mathbb{D}^n$ . For the sake of brevity, let us define the following symbols:

$$\Lambda \triangleq H^{-1}, \quad \hat{K} \triangleq KB^{-1}, \quad \hat{L} \triangleq LK^{-1}. \quad (41)$$

By considering (7), (40) can be rewritten as follows:

$$\dot{\hat{\sigma}} = \dot{e} + \Lambda(e - \dot{a}) + \hat{K}(\dot{a} + \hat{L}a) \quad (42a)$$

$$\ddot{a} = -\hat{K}(\dot{a} + \hat{L}a) + B^{-1}F \text{Sat}(F^{-1}B\hat{\sigma}) \quad (42b)$$

$$f = F \text{Sat}(F^{-1}B\hat{\sigma}), \quad (42c)$$

which is a multidimensional version of (19).

The whole robotic system is said to be in sliding mode if and only if  $s = 0$  is satisfied. From (42c), this condition is satisfied if  $x$  is included in the following set:

$$\mathcal{S} \triangleq \left\{ x \in \mathbb{R}^{4n} \mid |\hat{\sigma}_i| \leq \frac{F_i}{B_i} \quad \forall i \right\}. \quad (43)$$

Hereafter, we refer to  $\mathcal{S}$  as the *sliding region*. As long as  $x \in \mathcal{S}$ , the vector  $x$  evolves according to the differential equation  $s = 0$ , which is rewritten as follows:

$$\dot{q} = -\frac{q}{H} + \dot{p}_d + \frac{p_d}{H} \quad (44)$$

where we used  $q - p_d = -(e - \dot{a})$ . From this, one can see that the proxy position  $q$  is not influenced by any disturbances propagated through  $p$  as long as  $x \in \mathcal{S}$ . This property is inherited from the original concept of continuous-time SMC; it is lost in conventional discrete-time SMC, such as those using boundary layers.

### B. Convergence

The convergence property of the proposed control scheme is now analyzed. To represent the empirical fact that the PID control is useful for trajectory tracking of robotic systems, we set the following conjecture.

**Conjecture 1 (Local Passivity of the Well-Tuned PID Control):** Let us consider the system composed of the robot (37) and a PID controller (40c) that accepts an input  $u \triangleq \dot{q} - \dot{p}_d = \dot{a} - \dot{e} \in \mathbb{R}^n$ . Then, there exists a triplet of gain matrices  $B, K$ , and  $L \in \mathbb{D}^n$  that allows the existence of a function  $V_p : \mathbb{R}^{3n} \times \mathbb{R}^{n \times n} \rightarrow \mathbb{R}$ , a constant matrix  $\Xi \in \mathbb{R}^{n \times 3n}$ , and positive numbers  $\zeta, \delta, \rho_x$ , and  $\rho_u$  with which

$$V_p(x_e, M(p)) \geq \delta \|x_e\|^2 \quad (45)$$

holds for all  $x_e$  and  $p$ , and

$$\dot{V}_p(x_e, M(p)) \leq f^T u + \phi^T \Xi x_e - \rho_x \|x_e\|^2 - \rho_u \|u\|^2 \quad (46)$$

holds as long as  $\|C(p, \dot{p})\| < \zeta$  is satisfied.

As it is seen by setting  $u = \dot{e} = 0$ , this conjecture is a sufficient condition for the local asymptotic stability of PID set-point control, which has already been proven in the literature,

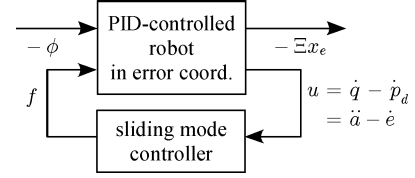


Fig. 6. Two-port network representation of a PID position-controlled robot and its interconnection with a sliding mode controller. (Because  $f$  and  $\dot{q}$  are related by a feed-through term, the causality between them can be reversed.)

e.g., [13] and [18]. The conjecture states that if the gains are appropriately chosen, the two-port network representation of the PID-controlled system illustrated in Fig. 6 is strictly passive and output-strictly passive [48] in a local sense. If the robot is strictly linear, as described in (11) (i.e.,  $\|C(p, \dot{p})\| = 0$ ), the system is implied to be globally passive.

Some of the Lyapunov functions for PID set-point control in the literature are candidates for the function  $V_p$ , but only strict Lyapunov functions, of which the time derivatives are strictly negative definite, may be used as  $V_p$ . Because such functions tend to be very complicated, as in, e.g., [18], we leave the validation of the conjecture outside the scope of this paper. The dependence of  $V_p$  on  $p$  is set to be only through  $M(p)$  so that the dependence of  $\dot{V}_p$  on  $\dot{p}$  is only through  $C(p, \dot{p})$  for the convenience of the analysis. This characteristic of  $V_p$  is shared with many Lyapunov functions of the PID-controlled robots in the literature, e.g., [6], [18], and [19].

The use of  $\Xi$  is to retain the generality of the conjecture, which is being inspired by the use of the output  $\dot{p} - \alpha \dot{a}$  (where  $\alpha$  is a positive constant) in the passivity analyses given by Arimoto [12, Sec. 3.2]. The condition  $\|C(p, \dot{p})\| < \zeta$  is introduced because the local nature of the stability of a PID-controlled robot is attributed to the nonlinear term  $C(p, \dot{p})$  [13].

Based on Conjecture 1, the stability of PSMC is shown as follows.

**Theorem 1 (Stability of PSMC):** Let us consider the system composed of (37) and (40) and assume that Conjecture 1 holds true. Also assume that the gain matrices  $K, B$ , and  $L$  are chosen as indicated in Conjecture 1, and that the diagonal elements of  $F$  are set sufficiently high. Then, there exists a closed set  $\mathcal{E}$  including the origin with which  $x \rightarrow \mathcal{E}$  is achieved as  $t \rightarrow \infty$  if there exists  $t_0 > 0$  with which  $\|C(p, \dot{p})\| < \zeta$  is satisfied for all  $t > t_0$ .

*Proof:* The system composed of (37) and (40) can be modeled as an interconnection of the PID-controlled system and a sliding mode controller, as illustrated in Fig. 6. Let us define

$$V(x, M(p)) \triangleq V_p(x_e, M(p)) + \|F(e - \dot{a})\|_1 \quad (47)$$

where  $x$  is the one that has been defined in (35). Then, because of (46), the following is satisfied:

$$\begin{aligned} \dot{V}(x, M(p)) &= \dot{V}_p(x_e, M(p)) + (\dot{e} - \ddot{a})^T F \text{Sgn}(e - \dot{a}) \\ &< -(\dot{e} - \ddot{a})^T (f - F \text{Sgn}(e - \dot{a})) \\ &\quad + \phi^T \Xi x_e - \rho_x \|x_e\|^2 - \rho_u \|u\|^2 \\ &\leq \phi^T \Xi x_e - \rho_x \|x_e\|^2 - \rho_u \|u\|^2 \\ &\leq \gamma_\phi \|\Xi\| \|x_e\| - \rho_x \|x_e\|^2 - \rho_u \|u\|^2 \end{aligned} \quad (48)$$

if  $\|C(p, \dot{p})\| < \zeta$ , where

$$\gamma_\phi \triangleq \alpha_0 + \zeta \gamma_v. \quad (49)$$

Here, we used the fact  $f = F \text{Sgn}(e - \dot{a} + H(\dot{e} - \ddot{a}))$  and the following property of Sgn function:

$$y^T X (\text{Sgn}(z + y) - \text{Sgn}(z)) \geq 0 \quad \forall z, y \in \mathbb{R}^n \quad \forall X \in \mathbb{D}^n.$$

We have also considered the bound of  $\phi$  in (39).

Because  $\ddot{a}$  is a function of  $x$ , as defined in (42b), we can define the following set in the state space:

$$\mathcal{E} \triangleq \{x \in \mathbb{R}^{4n} \mid \gamma_\phi \|\Xi\| \|x_e\| - \rho_x \|x_e\|^2 - \rho_u \|u\|^2 \geq 0\}. \quad (50)$$

Here,  $u = \ddot{a} - \dot{e}$  is a function of both  $x_e$  and  $e$  in  $x \in \mathcal{S}$ . Therefore, if the diagonal elements of  $F$  are set sufficiently high,  $\mathcal{E}$  is a closed set that satisfies  $0 \in \mathcal{E} \subset \mathcal{S}$ . Because  $\dot{V} \leq 0$  is satisfied outside the region  $\mathcal{E}$  as long as  $\|C(p, \dot{p})\| < \zeta$ ,  $x \rightarrow \mathcal{E}$  is satisfied as  $t \rightarrow \infty$  if there exists  $t_0 > 0$  with which  $\|C(p, \dot{p})\| < \zeta$  is satisfied for all  $t > t_0$ . ■

When PSMC is used for the set-point control and there is no disturbance (i.e., when  $\gamma_\phi = \alpha_0 = \gamma_v = 0$ ), the set  $\mathcal{E}$  shrinks to the origin ( $\mathcal{E} = \{0\}$ ). This means that the origin  $x = 0$  is locally asymptotically stable in this case. Global asymptotic stability is obtained for the strictly linear system (11), in which  $M(p)$  is a constant, and thus,  $C(p, \dot{p})$  is zero. For a nonlinear system (10), the stability is guaranteed only locally, and the system behaviors during the violation of the condition  $\|C(p, \dot{p})\| < \zeta$  cannot be predicted through the presented analysis. Determination of the region of attraction in this case is left outside the scope of this paper. Nonetheless, for any given  $x$ , the condition  $\|C(p, \dot{p})\| < \zeta$  can be satisfied by an appropriate design of  $p_d$  and  $\dot{p}_d$  because  $C(p, \dot{p})$  depends only on  $x$ ,  $p_d$ , and  $\dot{p}_d$ .

### C. Existence of the Sliding Mode

The existence of the sliding mode at the sliding region  $\mathcal{S}$  is now investigated. This property is necessary to achieve slow, overdamped resuming motion, which is characterized by the time-constant matrix  $H$ .

As shown in (43), the sliding region  $\mathcal{S}$  is defined by using the state-dependent vector  $\hat{\sigma}$ , which is defined in (42a). Its time derivative can be written as follows:

$$\begin{aligned} \dot{\hat{\sigma}} &= M(p)^{-1} \phi - M(p)^{-1} f + (\hat{K} - \Lambda) B^{-1} f \\ &\quad + (\Lambda - M(p)^{-1} (C(p, \dot{p}) + D)) \dot{e} \\ &\quad - (\hat{K} - \Lambda - \hat{L}) \hat{K} \dot{a} - (\hat{K} - \Lambda) \hat{K} \hat{L} a \\ &= -(M(p)^{-1} + \Lambda B^{-1}) f - \hat{K} (\hat{\sigma} - B^{-1} f) + \xi \end{aligned} \quad (51)$$

where

$$\begin{aligned} \xi(x, \phi, M(p), C(p, \dot{p})) &\triangleq M(p)^{-1} (\phi + (C(p, \dot{p}) + D) \dot{e}) \\ &\quad + \Lambda (-\dot{e} + \hat{K}(e + \hat{L}a)) + \hat{K}(\dot{e} + \hat{L}a) \in \mathbb{R}^n. \end{aligned} \quad (52)$$

By substituting (51) by (42c) and considering that  $\text{Dzn}(z) = z - \text{Sat}(z)$  for all  $z \in \mathbb{R}^n$ , we obtain

$$\begin{aligned} \dot{\hat{\sigma}} &= -(M(p)^{-1} + \Lambda B^{-1}) F \text{Sat}(BF^{-1} \hat{\sigma}) \\ &\quad - \hat{K} B^{-1} F \text{Dzn}(BF^{-1} \hat{\sigma}) + \xi. \end{aligned} \quad (53)$$

Now, let us define the function  $U : \mathbb{R}^n \rightarrow \mathbb{R}$  as follows:

$$U(\hat{\sigma}) \triangleq \|F^2 B^{-1} \text{Dzn}(BF^{-1} \hat{\sigma})\|_1, \quad (54)$$

with which  $U(\hat{\sigma}(x)) = 0$  is equivalent to  $x \in \mathcal{S}$ . Because

$$\frac{\partial \|X \text{Dzn}(z)\|_1}{\partial z^T} = X \text{Dsg}(z) \quad \forall X \in \mathbb{D}^n \quad \forall z \in \mathbb{R}^n, \quad (55)$$

the time derivative of  $U(\hat{\sigma})$  can be written as follows:

$$\begin{aligned} \dot{U}(\hat{\sigma}) &= \text{Dsg}(BF^{-1} \hat{\sigma})^T F \dot{\hat{\sigma}} \\ &< -\text{Dsg}(BF^{-1} \hat{\sigma})^T F (WF \text{Sat}(BF^{-1} \hat{\sigma}) \\ &\quad + \hat{K} F B^{-1} \text{Dzn}(BF^{-1} \hat{\sigma}) - \xi) \\ &< -\sum_{i=1}^n |c_i(x)| F_i (W_i F_i - c_i(x) \xi_i) \end{aligned} \quad (56)$$

where

$$c_i(x) \triangleq \text{dsg}\left(\frac{\hat{\sigma}_i(x)}{F_i/B_i}\right) \in \mathbb{R} \quad (57)$$

$$W \triangleq M_{\max}^{-1} + \Lambda B^{-1} \in \mathbb{D}^n \quad (58)$$

and  $M_{\max} \in \mathbb{D}^n$  is a positive-definite diagonal matrix with which  $M_{\max} - M(p)$  is positive definite for all  $p \in \mathbb{R}^n$ . Here, we used the facts that  $\text{dsg}(z) = |\text{dsg}(z)| \text{dsg}(z)$ ,  $\text{dsg}(z) \text{sat}(z) = |\text{dsg}(z)|$ , and  $\text{dsg}(z) \text{dzn}(z) = |\text{dzn}(z)|$  for all  $z \in \mathbb{R}$ .

From (56),  $\dot{U} \leq 0$  is satisfied on the set  $\mathcal{D}$  that is defined as follows:

$$\begin{aligned} \mathcal{D}(\phi, M(p), C(p, \dot{p})) &\triangleq \left\{x \in \mathbb{R}^{4n} \mid \|\xi(x, \phi, M(p), C(p, \dot{p}))\| \right. \\ &\quad \left. < \min_{i \in \{1, \dots, n\}} W_i F_i \right\}. \end{aligned} \quad (59)$$

Now, we are in position to show the existence of the sliding mode.

*Theorem 2 (Existence of the Sliding Mode):* Let us consider the system composed of (37) and (40), and assume that Conjecture 1 holds true. Assume that the gain matrices  $K$ ,  $B$ , and  $L$  are chosen as indicated in Conjecture 1, and that  $F_i$  are set sufficiently high. In addition, assume that  $\|C(p, \dot{p})\| < \zeta$  is satisfied for all  $t > 0$ . Then, there exist  $t_d > 0$  and  $t_s > t_d$  with which  $x \in \mathcal{D} \cap \bar{\mathcal{S}} \forall t \in (t_d, t_s)$  and  $x \in \mathcal{D} \cap \mathcal{S} \forall t \in (t_s, \infty)$ , where the bar denotes the complementary set.

*Proof:* From the definition of  $\xi$  in (52) and the assumption  $\|C(p, \dot{p})\| < \zeta$ , it is clear that  $\mathcal{E} \subset \mathcal{D}$  is satisfied if  $F_i$  are chosen sufficiently high. Therefore, Theorem 1 implies that there exists  $t_d > 0$  with which  $x \in \mathcal{D} \forall t \in (t_d, \infty)$ , if Conjecture 1 is correct. After realizing  $x \in \mathcal{D}$  at  $t > t_d$ , considering that  $\dot{U} < 0$  if  $x \in \mathcal{D} \cap \bar{\mathcal{S}}$  and  $\dot{U} = 0$  if  $x \in \mathcal{S}$ , there exists  $t_s > t_d$  with which  $x \notin \mathcal{S} \forall t < t_s$  and  $x \in \mathcal{S} \forall t > t_s$ . ■

Theorem 2 means that the sliding mode occurs in  $\mathcal{S}$  after  $x \in \mathcal{D}$  is achieved.

The conclusion drawn from the analysis in this section is that PSMC (40), of which the discrete-time representation is given in (32), drives the nonlinear robotic system (10) to  $\mathcal{E}$ , which is the neighborhood of the origin, at which  $q = p = p_d$ ,  $\dot{p} = \dot{p}_d$ , and  $a = 0$ , if the parameters ( $K$ ,  $B$ ,  $L$ , and  $F$ ) are appropriately chosen, if  $\dot{p}_d$ ,  $\dot{p}_d$ , and  $h$  are bounded, and if  $\|C(p, \dot{p})\|$  is always

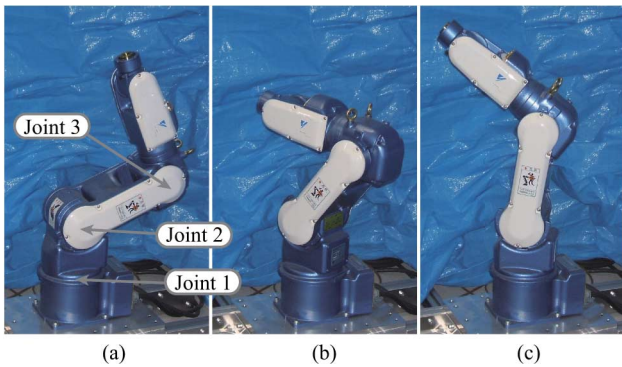


Fig. 7. Six degree-of-freedom manipulator used in the experiments. (a) Configuration A ( $[0, -70, 0]^\circ$ ). (b) Configuration B ( $[-60, -40, 30]^\circ$ ). (c) Configuration C ( $[-30, -10, -30]^\circ$ ).

TABLE I  
CONTROLLER PARAMETERS FOR THE JOINTS

parameter (unit)	Joint 1	Joint 2	Joint 3
torque limit: $F$ (Nm)	30	55	30
P-gain: $K$ (N/m)	10000	20000	10000
D-gain: $B$ (Ns/m)	20	40	20
I-gain: $L$ (N/ms)	20000	40000	20000

small enough. Before reaching the neighborhood of the origin, the system reaches a set  $\mathcal{D}$  including  $\mathcal{E}$ , and following this, the system is attracted to the sliding region  $\mathcal{S}$ . During the sliding mode, the proxy position  $q$  exponentially moves toward the desired position  $p_d$  without being influenced by disturbances.

## VI. EXPERIMENTS

The presented technique was experimentally tested by using the 6-DOF industrial manipulator MOTOMAN-UPJ (Yaskawa Electric Corporation) shown in Fig. 7, which was controlled through a PC running the ART-Linux operating system. This manipulator had six actuators, which were AC servomotors integrated with harmonic-drive gearings and optical encoders. Each joint was controlled with the use of PSMC [(32) or (33)], PID control with a simple torque limiter, or PID control with antiwindup compensation presented in [35]. In the experiment, only the first three joints (from the base) were used, and the other joints were controlled to maintain a constant angle with the use of the controller (32). The gear ratios of the first three joints were 100, 192, and 120.

The time-step size (sampling interval) of the controllers was  $T = 0.001$  s. The time constant  $H$  of PSMC was assigned some different values in the experiments. The other parameters for PSMC were chosen as shown in Table I. The PID gains ( $K$ ,  $L$ , and  $B$ ) were chosen by trial and error to realize as accurate and stiff angle control as possible. This trial-and-error gain tuning was performed in the same manner as that for the conventional PID control because PSMC is equivalent to the conventional PID control when the actuators are not saturated. The torque limits  $F$  were also chosen by trial and error so that the actuators do not saturate during the tracking of smooth desired trajectories given in the experiment.

We did not attempt to relate the chosen parameters to the stability analysis given in Section V because the analysis

depends on an unproven property of PID-controlled robots, and it provides no explicit guidelines for the choice of parameters. It would be difficult to check whether the manipulator inertia matrix and the gains matrices satisfy the conditions that were described in Conjecture 1. It would require an appropriate expression of the function  $V_p$  to be found, and even if it is found, it would be very complicated. Such an analysis is concerned with the conventional PID control, and thus falls outside the scope of this paper.

No attempts were made to include the original SMC law (without a boundary layer) into the comparison because it is known to be unpractical due to its tendency to exhibit chattering. No comparisons were either made to control schemes aiming for better control performance, such as adaptive controllers, because the main purpose of PSMC is to ensure safety while maintaining the accuracy of PID control. I-PD control was not compared because it is known to have lower tracking capability than PID control.

### A. Set-Point Control

A set of experiments were performed to show the resuming motion from large positional (angular) errors, which can be produced when discontinuous desired angles are provided as in set-point control and when there are large external forces. The desired angles were changed among the three configurations shown in Fig. 7. To be specific, the initial angles of the first three joints were chosen as configuration A in Fig. 7. The desired angles were discontinuously changed to configuration B at  $t = 1$  s, then to configuration C at  $t = 4$  s, and finally, again to configuration A at  $t = 7$  s. Each joint was controlled by using the control law (32). Three trials were performed with different  $H$  values:  $H = 0.1, 0.2$ , and  $0.4$  s.

The angle and torque profiles from joint 2 under the three values of  $H$  are shown in Fig. 8. The results indicate that the joints properly exhibit overdamped, exponential resuming motion toward desired angles. In practical situations, this property can be considered beneficial for safety. Different  $H$  values were used to demonstrate their effects on the speed of the convergent behavior. As the  $H$  value decreases, the speed of the motion increases, which results in longer periods of saturation in the actuator torques.

Another set of trials were performed to compare PSMC to two conventional variants of PID control: PID control with simple torque limits and antiwindup PID control shown by [35, eq. (7)] (with  $\gamma = 0.5$ ). The gains and the torque limits for the conventional controllers were chosen as Table I. With torque-limited PID control, the desired angle commands used in Fig. 8 produced emergency stop in the servo amplifier of the AC servomotors due to the excessive speed of the joints. Thus, only  $15^\circ$  of discontinuities were applied to the joints as desired angle commands. Data from all joints are shown in Fig. 9. The results clearly show that PSMC is effective in removing overshoots and oscillations, which are produced with torque-limited PID control. It is shown that antiwindup PID control may or may not succeed in suppressing overshoots and oscillation and that its resultant motion strongly depends on controlled objects. This

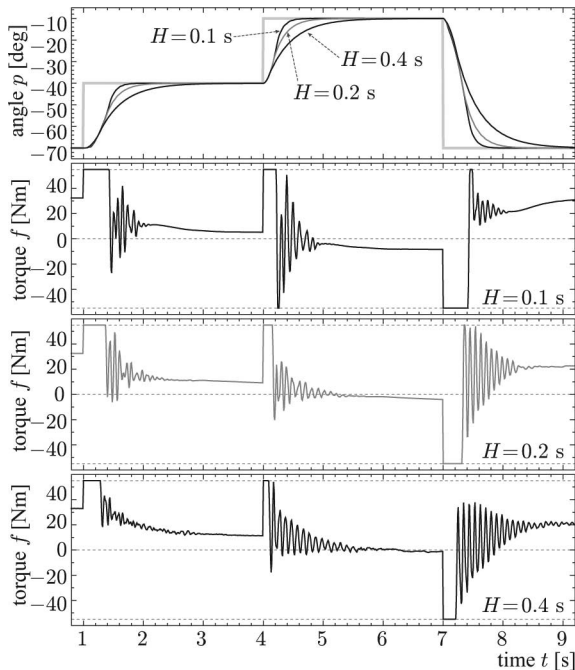


Fig. 8. Data from joint 2 during set-point control under PSMC with different  $H$  values. The thick gray plot indicates the desired angle  $p_d$ .

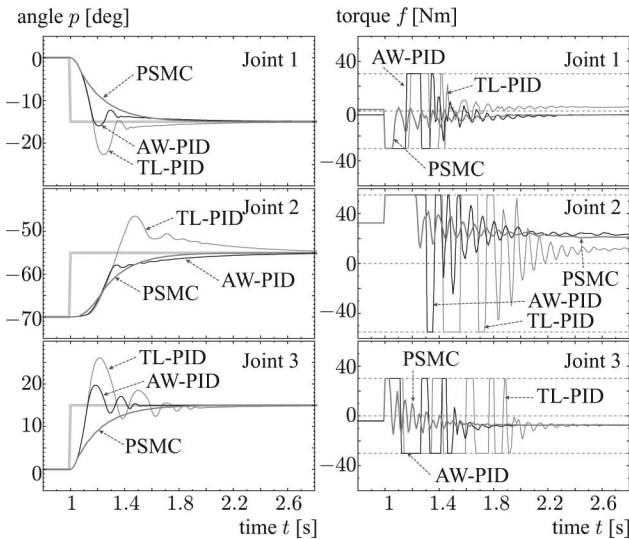


Fig. 9. Data from all joints during set-point control under torque-limited PID (TL-PID), anti-windup PID (AW-PID), and PSMC with  $H = 0.2$  s. The thick gray plots indicate the desired angles  $p_d$ .

feature can prevent a straightforward adjustment of the postsaturation behavior. In contrast, PSMC always produces exponential motions, of which slowness can be explicitly adjusted by the parameter  $H$ .

### B. Trajectory-Tracking Control

Another set of experiments were performed to show the behavior of PSMC during trajectory-tracking control. Sinusoidal desired-angle trajectories with an amplitude of  $60^\circ$  and a cycle of 3 s were provided to the joints. The trajectories start from

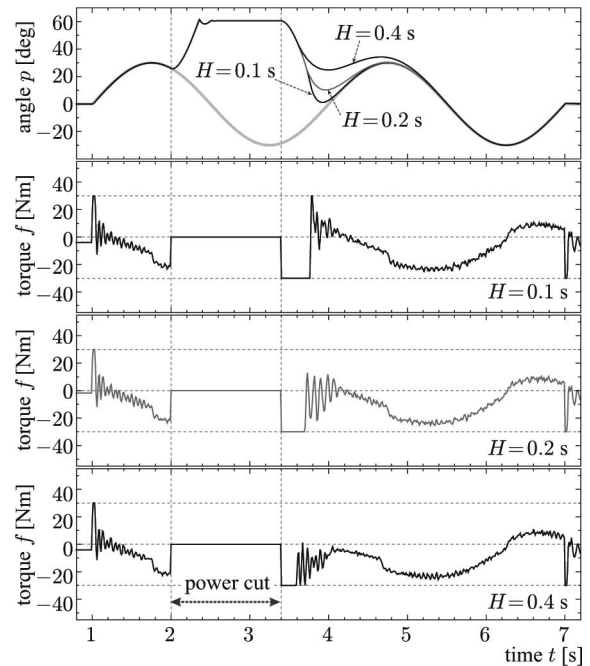


Fig. 10. Data from joint 3 during trajectory-tracking control under PSMC with different  $H$  values. The actuator torques were cut off from  $t = 2$  s to  $3.4$  s, during which the joint moved due to the gravity. The thick gray plot indicates the desired angle  $p_d$ .

the configuration A at  $t = 1$  s and pass through the two other configurations. In addition, the actuator torques were forced to be zero from  $t = 2$  to  $3.4$  s to simulate a temporary power failure and large positional (angular) errors.

The results obtained from joint 3 are shown in Fig. 10. It shows that the joint angle exponentially converges to the desired trajectory after the power recovery at  $t = 3.4$  s, and the speed of the convergence can be adjusted by the value of  $H$ . As mentioned with the results under set-point control, this property produces safer behavior in such cases as unexpected contacts with external objects.

A comparison was made with the PID control to compare the control performance. The aforementioned sinusoidal desired trajectory was also used for conventional PID control with torque limiter and PSMC with  $H = 0.2$  s. The power cut was not performed because, under PID control, it produced excessive speed that resulted in an emergency stoppage of the servo amplifiers. The results, shown in Fig. 11, indicate that the errors remaining under PSMC are almost of the same level as those under torque-limited PID control. Differences appear only after torque saturations. An angular error produced by torque saturation is recovered quickly with PID control; however, it can produce overshoots and excessive speeds, which are usually considered unsafe in practical situations.

The effect of the integral action [PID-type PSMC (32) as opposed to PD-type PSMC (33)] was tested by performing another trial by the control law (33). The same sinusoidal input with a power-cut period was provided to the joints. The parameters for the PD-type PSMC (33) were chosen as Table I and  $H = 0.2$  s, except  $L$  was not used. Fig. 12 shows the data from this trial and

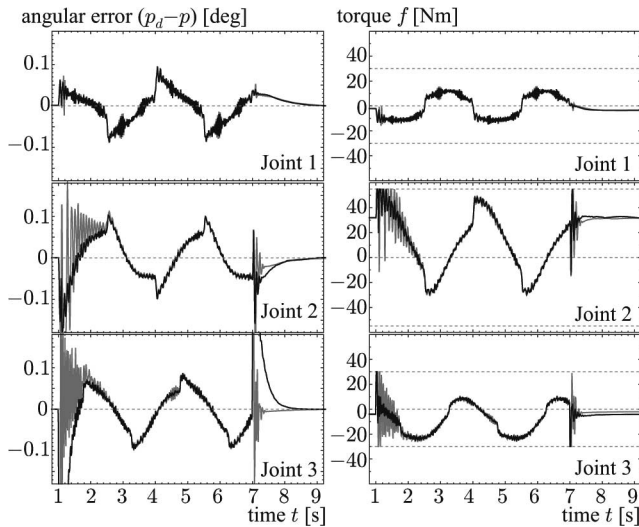


Fig. 11. Data from all joints during trajectory-tracking control under (gray) torque-limited PID control and (black) PSMC with  $H = 0.2$  s.

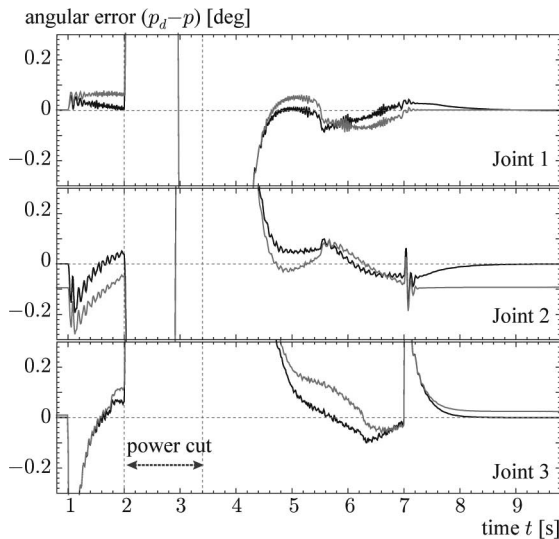


Fig. 12. Data from all joints during trajectory-tracking control with a temporal power cut (2–3.4 s) under (black) PID-type PSMC (32) and (gray) PD-type PSMC (33).

the correspondent trial with PID-type PSMC, a part of which is already shown in Fig. 10. The results show that PID-type PSMC is effective to remove steady-state errors, which can be produced with PD-type PSMC under the gravity and joint friction. This is, indeed, a well-known advantage of conventional PID control over conventional PD control. The present results indicate that this property is also preserved in the framework of PSMC.

## VII. CONCLUSION

This paper has proposed PSMC for the position control of robotic manipulators. The proposed method is an alternative discrete-time approximation of a class of SMC and is also an extension of the PID control. The method is safer than and as accurate as PID position control; PSMC is capable of producing overdamped resuming motion from large positional errors

without sacrificing tracking accuracy during normal operation. The method is suited for situations where large positional errors that accompany actuator-force saturation are probable due to unexpected environment contact and/or nonsmooth position commands.

It must be noted that the presented stability analysis on a robot under PSMC depends on a conjecture of the local passivity of a PID-controlled robot. The validation of the conjecture remains an important issue for future study.

After Kikuuwe and Fujimoto's initial disclosure of PSMC in 2006 [1], it has been reported that this scheme was successfully utilized with pneumatic actuators [49]. Besides, it has been experimentally shown that the slow resuming motion realized with PSMC is suited for some classes of human-machine coordination [8]. The method can be used as a lowest level servo loop for more sophisticated control schemes, such as admittance control, which has been used by Kikuuwe *et al.* [9].

This paper has limited itself to 1-D PSMC, which can be used for decentralized joint-angle control. Many variants and extensions are, however, expected to be drawn from PSMC. One straightforward extension is to combine PSMC with other compensation terms, such as gravity compensation, as already demonstrated with pneumatic actuators [49]. Another imaginable variation is multidimensional PSMC for task-space position control, which has been empirically demonstrated [1], [8], [49], although its theoretical validity has not been fully discussed. In addition, Kikuuwe *et al.* have proposed an extension of PSMC to impose limits on the end-effector Cartesian velocity [7], of which the stability analysis is left unfinished. From a theoretical point of view, a more general mathematical framework that includes PSMC as a special case can be considered as a future topic of study. In such a framework, conventional sliding mode controllers might be converted into chattering-free discrete-time controllers by algebraically combining them with simpler controllers, such as a PID controller.

## REFERENCES

- [1] R. Kikuuwe and H. Fujimoto, "Proxy-based sliding mode control for accurate and safe position control," in *Proc. IEEE Int. Conf. Robot. Autom.*, 2006, pp. 26–31.
- [2] P. Rocco, G. Ferretti, and G. Magnani, "Implicit force control for industrial robots in contact with stiff surfaces," *Automatica*, vol. 33, no. 11, pp. 2041–2047, 1997.
- [3] R. Q. Van Der Linde, P. Lammertse, E. Frederiksen, and B. Ruiters, "The HapticMaster, a new high-performance haptic interface," in *Proc. 2nd Eurohaptics*, 2002, pp. 1–5.
- [4] I. Cervantes and J. Alvarez-Ramirez, "On the PID tracking control of robot manipulators," *Syst. Control Lett.*, vol. 42, pp. 37–46, 2001.
- [5] P. Rocco, "Stability of PID control for industrial robot arms," *IEEE Trans. Robot. Autom.*, vol. 12, no. 4, pp. 606–614, Aug. 1996.
- [6] S. Arimoto and F. Miyazaki, "Stability and robustness of PID feedback control for robot manipulators of sensory capability," in *Proc. First Int. Symp. Robot. Res.*, M. Brady and R. Paul, Eds. Cambridge, MA: MIT Press, 1984, pp. 783–799.
- [7] R. Kikuuwe, T. Yamamoto, and H. Fujimoto, "Velocity-bounding stiff position controller," in *Proc. IEEE/RSJ Int. Conf. Intell. Robots Syst.*, Oct. 2006, pp. 3050–3055.
- [8] R. Kikuuwe, T. Yamamoto, and H. Fujimoto, "A guideline for low-force robotic guidance for enhancing human performance of positioning and trajectory tracking: It should be stiff and appropriately slow," *IEEE Trans. Syst., Man, Cybern. A, Syst., Humans*, vol. 38, no. 4, pp. 945–957, Jul. 2008.

- [9] R. Kikuuwe, N. Takesue, and H. Fujimoto, "A control framework to generate nonenergy-storing virtual fixtures: Use of simulated plasticity," *IEEE Trans. Robot.*, vol. 24, no. 4, pp. 781–793, Aug. 2008.
- [10] Y. J. Looftma, A. J. Van der Schaft, and M. K. Çamlbel, "Uniqueness of solutions of linear relay systems," *Automatica*, vol. 35, pp. 467–478, 1999.
- [11] M. K. Çamlbel, W. P. M. H. Heemels, and J. M. Schumacher, "Consistency of a time-stepping method for a class of piecewise-linear networks," *IEEE Trans. Circuits Syst. I, Fundam. Theory Appl.*, vol. 49, no. 3, pp. 349–357, Mar. 2002.
- [12] S. Arimoto, *Control Theory of Nonlinear Mechanical Systems: A Passivity-Based and Circuit-Theoretic Approach*. London, U.K.: Oxford Univ. Press, 1996.
- [13] R. Kelly, V. Santibáñez, and A. Loría, *Control of Robot Manipulators in Joint Space*. New York: Springer-Verlag, 2005.
- [14] M. Takegaki and S. Arimoto, "A new feedback method for dynamic control of manipulator," *Trans. ASME, J. Dyn. Syst. Meas. Control*, vol. 102, pp. 109–125, 1981.
- [15] S. Kawamura, F. Miyazaki, and S. Arimoto, "Is a local linear pd feedback control law effective for trajectory tracking?" in *Proc. IEEE Int. Conf. Robot. Autom.*, 1988, pp. 1335–1340.
- [16] X. Wang and L.-K. Chen, "Proving the uniform boundedness of some commonly used control schemes for robots," in *Proc. IEEE Int. Conf. Robot. Autom.*, 1989, pp. 1491–1496.
- [17] Z. Qu and J. Dorsey, "Robust tracking control of robots by a linear feedback law," *IEEE Trans. Autom. Control*, vol. 36, no. 9, pp. 1081–1084, Sep. 1991.
- [18] J. T. Wen and S. H. Murphy, "PID control for robot manipulators," CIRSSE Document #54, Rensselaer Polytechnic Inst., Troy, NY, May 1990.
- [19] R. Kelly, "A tuning procedure for stable PID control of robot manipulators," *Robotica*, vol. 13, no. 2, pp. 141–148, 1995.
- [20] B. Armstrong and B. Amin, "PID control in the presence of static friction: A comparison of algebraic and describing function analysis," *Automatica*, vol. 32, no. 5, pp. 679–692, 1996.
- [21] J. Alvarez-Ramirez, R. Kelly, and I. Cervantes, "Semiglobal stability of saturated linear PID control for robot manipulators," *Automatica*, vol. 39, no. 6, pp. 989–995, 2003.
- [22] J. Alvarez-Ramirez, V. Santibáñez, and R. Campa, "Stability of robot manipulators under saturated PID compensation," *IEEE Trans. Control Syst. Technol.*, vol. 16, no. 6, pp. 1333–1341, Nov. 2008.
- [23] K. Watanabe, H. Nagayasu, N. Kawakami, and S. Tachi, "Mechanical compliance control system for a pneumatic robot arm," in *Proc. SICE Annu. Conf.*, 2008, pp. 2789–2794.
- [24] K. Hoshino, "Control of speed and power in a humanoid robot arm using pneumatic actuators for human-robot coexisting environment," *IEICE Trans. Inf. Syst.*, vol. E91-D, no. 6, pp. 1693–1699, 2008.
- [25] S.-T. Wu, "Digital high-gain PD control of robot manipulators," *J. Robotic Systems*, vol. 14, no. 5, pp. 375–387, 1997.
- [26] R. Marino, "High-gain feedback in non-linear control systems," *Int. J. Control*, vol. 42, no. 6, pp. 1369–1385, 1985.
- [27] K.-K. D. Young, P. V. Kokotovic, and V. I. Utkin, "A singular perturbation analysis of high-gain feedback systems," *IEEE Trans. Autom. Control*, vol. 22, no. 6, pp. 931–939, Dec. 1977.
- [28] J.-J. E. Slotine and S. S. Sastry, "Tracking control of non-linear systems using sliding surfaces, with application to robot manipulators," *Int. J. Control*, vol. 38, no. 2, pp. 465–492, 1983.
- [29] F. Janabi-Sharifi, V. Hayward, and C.-S. J. Chen, "Discrete-time adaptive windowing for velocity estimation," *IEEE Trans. Control Syst. Technol.*, vol. 8, no. 6, pp. 1003–1009, Nov. 2000.
- [30] V. Parra-Vega, S. Arimoto, Y.-H. Liu, G. Hirzinger, and P. Akella, "Dynamic sliding PID control for tracking of robot manipulators: Theory and experiments," *IEEE Trans. Robot. Autom.*, vol. 19, no. 6, pp. 967–976, Dec. 2003.
- [31] Y.-S. Lu, "Integral variable-structure control with variable-structure sliding dynamics for antireset windup," *Proc. Inst. Mechanical Engineers Part I, J. Syst. Control Eng.*, vol. 222, no. 3, pp. 209–216, 2008.
- [32] R. Hanus, M. Kinnaert, and J.-L. Henrotte, "Conditioning technique, a general anti-windup and bumpless transfer method," *Automatica*, vol. 23, no. 6, pp. 729–739, 1987.
- [33] K. S. Walgama, S. Rönnbäck, and J. Sternby, "Generalisation of conditioning technique for anti-windup compensators," *Proc. Inst. Electr. Eng—Control Theory Appl.*, vol. 139, no. 2, pp. 109–118, 1991.
- [34] M. V. Kothare, P. J. Campo, M. Morari, and C. N. Nett, "A unified framework for the study of anti-windup designs," *Automatica*, vol. 30, no. 12, pp. 1869–1883, 1994.
- [35] Y. Li, K. H. Ang, and G. C. Y. Chong, "PID control system analysis and design," *IEEE Control Syst. Mag.*, vol. 26, no. 1, pp. 32–41, 2006.
- [36] A. Bemporad, "Reference governor for constrained nonlinear systems," *IEEE Trans. Autom. Control*, vol. 43, no. 3, pp. 415–419, Mar. 1998.
- [37] E. Gilbert and I. Kolmanovsky, "Nonlinear tracking control in the presence of state and control constraints: A generalized reference governor," *Automatica*, vol. 38, no. 12, pp. 2063–2073, 2002.
- [38] A. S. Hodel and C. E. Hall, "Variable-structure PID control to prevent integrator windup," *IEEE Trans. Ind. Electron.*, vol. 48, no. 2, pp. 442–451, Apr. 2001.
- [39] A. Visioli, "Modified anti-windup scheme for PID controllers," *Proc. Inst. Electr. Eng—Control Theory Appl.*, vol. 150, no. 1, pp. 49–54, 2003.
- [40] P. Dworkin and D. Zeltzer, "A new model for efficient dynamic simulation," in *Proc. 4th Eurograph. Workshop Animation Simul.*, 1993, pp. 135–147.
- [41] C. B. Zilles and J. K. Salisbury, "A constraint-based god-object method for haptic display," in *Proc. IEEE/RSJ Int. Conf. Intell. Robots Syst.*, 1995, pp. 146–151.
- [42] D. C. Ruspini, K. Kolarov, and O. Khatib, "The haptic display of complex graphical environments," in *Proc. ACM SIGGRAPH*, 1997, pp. 345–352.
- [43] J. E. Colgate, M. C. Stanley, and J. M. Brown, "Issues in the haptic display of tool use," in *Proc. IEEE/RSJ Int. Conf. Intell. Robots Syst.*, 1995, vol. 3, pp. 140–145.
- [44] J.-J. E. Slotine, "The robust control of robot manipulators," *Int. J. Robot. Res.*, vol. 4, no. 2, pp. 49–63, 1985.
- [45] K. S. Yeung and Y. P. Chen, "A new controller design for manipulators using the theory of variable structure systems," *IEEE Trans. Autom. Control*, vol. 33, no. 2, pp. 200–206, Feb. 1988.
- [46] S.-T. Wu, "On digital high-gain and sliding-mode control," *Int. J. Control*, vol. 66, no. 1, pp. 65–84, 1997.
- [47] J. G. Ziegler and N. B. Nichols, "Optimum settings for automatic controllers," *Trans. ASME*, vol. 64, pp. 759–768, 1942.
- [48] H. K. Khalil, *Nonlinear Systems*, 3rd ed. Englewood Cliffs, NJ: Prentice-Hall, 2002.
- [49] M. Van Damme, B. Vanderborght, B. Verrelst, R. Van Ham, F. Daerden, and D. Lefeber, "Proxy-based sliding mode control of a planar pneumatic manipulator," *Int. J. Robot. Res.*, vol. 28, no. 2, pp. 266–284, 2009.



**Ryo Kikuuwe** (S'02–M'03) received the B.S., M.S., and Ph.D.(Eng.) degrees from Kyoto University, Kyoto, Japan, in 1998, 2000, and 2003, respectively, all in mechanical engineering.

From 2003 to 2007, he was an Endowed-Chair Research Associate with Nagoya Institute of Technology, Nagoya, Japan. He is currently an Associate Professor with the Department of Mechanical Engineering, Kyushu University, Fukuoka, Japan. His research interests include human–robot coordination, real-time simulation for haptic rendering and physics-

based animation, and tactile sensing.

Prof. Kikuuwe is a member of the Robotics Society of Japan, the Japan Society of Mechanical Engineers, the Society of Instrument and Control Engineers of Japan, and the Virtual Reality Society of Japan.



**Satoshi Yasukouchi** received the B.E. and M.E. degrees from Kyushu University, Fukuoka, Japan, in 2008 and 2010, respectively, all in mechanical engineering.

He was with the Department of Intelligent Machinery and Systems, Kyushu University. He is currently with Yaskawa Electric Corporation, Kitakyushu, Japan.



**Hideo Fujimoto** received the B.E. and Dr. Eng. degrees from Nagoya University, Nagoya, Japan, in 1970 and 1982, respectively, all in mechanical engineering.

He is currently a Professor with Nagoya Institute of Technology. His research interests include medical engineering, haptic engineering, and robotics.

Prof. Fujimoto is a Fellow of the Japan Society of Mechanical Engineers. He was the Chair Person of the Aichi Prefecture Manufacturing Personnel Training Meeting, a member of the Committee on Cultural

Resources of the Council for Science and Technology of the Ministry of Education, Culture, Sports, Science, and Technology of Japan, and the President of the Scheduling Society of Japan. He was the recipient of the Best Paper Award for a paper presented at the 2000 Japan-USA Flexible Automation Symposium, the Best Paper Award at the Sixth Robotics Symposium, the Contribution Award from the System Integration Section, Society of Instrument and Control Engineers, and the Great Contribution Award from the Production System Section, the Japan Society of Mechanical Engineers, in 2002.



**Motoji Yamamoto** (M'02) received the B.E., M.S., and Dr. Eng. degrees from Kyushu University, Fukuoka, Japan, in 1985, 1987, and 1990, respectively, all in mechanical engineering.

In 1990, he joined the Department of Intelligent Machinery and Systems, Kyushu University, as a Lecturer, where he was an Associate Professor and a Professor, in 1992 and 2005, respectively. He is currently with the Department of Mechanical Engineering, Kyushu University. His research interests include field and service robots, parallel-wire mechanisms,

human care, and medical robots.